For reprint orders, please contact:
reprints@futuremedicine.com

REVIEW

Delivery of nano-objects to functional sub-domains of healthy and failing cardiac myocytes

Valeriy Lukyanenko
University of Maryland Biotechnology Institute, Medical Biotechnology Center, 725 W. Lombard St., Rm S216, Baltimore, MD 21201, USA
Tel.: +1 410 706 8559;
Fax: +1 410 706 8184;
Email: lukyanen@umbi.umd.edu

Cardiovascular disease, including heart failure, is one of the leading causes of mortality in the world. Delivery of nano-objects as carriers for markers, drugs or therapeutic genes to cellular organelles has the potential to sharply increase the efficiency of diagnostic and treatment protocols for heart failure. However, cardiac cells present special problems to the delivery of nano-objects, and the number of papers devoted to this important area is remarkably small. The present review discusses fundamental aspects, problems and perspectives in the delivery of nano-objects to functional sub-domains of failing cardiomyocytes. What size nano-objects can reach cellular sub-domains in failing hearts? What are the mechanisms for their permeation through the sarcolemma? How can we improve the delivery of nano-objects to the sub-domains? Answering these questions is fundamental to identifying cellular targets within the failing heart and the development of nanocarriers for heart-failure therapy at the cellular level.

Keywords: cardiac myocyte, cardiac nanomedicine, diffusion pathways, drug and gene delivery, nanocarriers, nanoparticles

future medicine part of fsg

One of the most exciting areas of nanobiotechnology is the use of nano-objects to carry out specific functions. Nano-objects can be used in a variety of biomedical and biotechnological applications, including drug and therapeutic gene delivery [1–15].

Cardiovascular disease is one of the leading causes of mortality in the world according to the WHO. Targeted delivery of analytic probes and therapeutic agents to cardiac myocytes and cellular compartments could significantly increase the efficiency of both diagnostic and treatment protocols for heart failure and could also have a significant impact on US morbidity. However, the field of cardiac nanomedicine remains virtually undeveloped and basic questions remain to be elucidated.

There are three major problems in the field:

- Which drugs, markers and genes are to be used;
- How to fabricate suitable nanocarriers;
- How to deliver the nano-objects to their targets.

Solutions for every one of these problems are in the embryonic stage. However, the solutions for the first two problems depend very much on the third. On the way to their cardiac targets, nano-objects must penetrate through capillary barriers, the sarcolemma and multiple intracellular barriers, which are unique to the structure of cardiac myocytes [16]. The size of the carrier must enable it to reach the target and coatings have to facilitate transportation through the cellular membrane. Here, we analyze for the first time the literature relevant to the most fundamental questions for the development of cardiac nanomedicine:

- The actual clearance of the pathways for nano-objects within the heart and ventricular myocytes;
- The possible barriers for nano-objects;
- The mechanisms for their permeation into healthy and failing cardiac myocytes.

For nanotechnology involved in the therapy of vascular problems resulting in heart failure, readers are directed to the reviews by Kong and Goldschmidt-Clermont and Brewster *et al.* [10,12].

Nano-objects in biomedical research

The diagnosis and treatment of disease at the cellular level would be enhanced greatly by the ability to deliver analytic probes and therapeutic agents into specific cells and cellular compartments. The potential benefits of using nano-objects are expected to lead to an expanded range of applications in future biological research, diagnostics and therapy [17]. All nanostructures with important analytical applications could be divided into two groups:

- Nano-objects (nanotubes, inorganic nanocrystals, spherical nanoparticles, nanorods, nanoprisms and macromolecules)
- Nanodevices (nanocapacitors, nanopores and nanocantilevers) [5,17,8,12,18].

Nano-objects can be used in a variety of bioanalytical formats:

- As quantitative tags, such as the optical detection of quantum dots and the electrochemical detection of metallic nanoparticles;
- As substrates for multiplexed bioassays (encoded nanoparticles, such as striped metallic nanoparticles);
- As controllers of signal transduction (e.g., in colloidal gold-based aggregation assays);
- As catalyzers or inducers of biological processes (i.e., nonviral vectors).

Chemotherapeutic and imaging nano-objects are usually conjugated to the chemotherapeutic drug (i.e., paclitaxel or doxorubicin) and/or imaging agent (fluorescein isothiocyanate [FITC] or green fluorescent protein [GFP]) [7,19]. The next generation of nano-objects, nanodots and carbon nanotubes are expected to be used in the life sciences [1,3,8]. However, engineering useful nano-objects includes understanding how they can get to their expected targets. This requires knowing all the cellular and subcellular pathways, possible barriers and transport mechanisms to the intended cellular or subcellular target.

Nano-objects, which have been suggested for biomedical research, have diameters from 0.8 to 200 nm [1,3,4,7,13,14,17,20–22,]. However, only nano-objects ≤100 nm are optimal for intravenous injection [4,23]. The pathway for nano-objects to target an intracellular sub-domain *in vivo* includes three steps:

- Diffusion from capillaries to the cell surface;
- Permeation through the sarcolemma;
- Diffusion around barriers within the cell.

Although the potential benefits of using nano-objects point to an expanded range of applications in future biological research, diagnostics and therapy, little is known about the actual constraints of diffusion pathways for nano-objects within organs and cells.

Constraints in delivery of nano-objects from capillary to cardiac cells

One of the most critical issues for successful nano-object delivery includes the ability of the nano-objects to penetrate through the barrier of the continuous microvascular endothelium. Some research data show that the capillary barrier is 'transparent' only for particles ≤50 nm [1,24,25]. However, data about size constraints for delivery of nano-objects to heart cells are very limited. Measurements of the levels of doxorubicin in murine tissues after intravenous injections of 15–30 nm nanoparticles incorporating doxorubicin showed that they can be accumulated in tumors, liver and spleen, but not in the heart, kidneys and lungs [7]. In addition, recently, Vancraeynest *et al.* [26] infused 30 and 100 nm fluorescent nanospheres intravenously but did not find them within the rat myocardium under control conditions. To deliver these nano-objects to cardiac cells, the authors had to develop a new method: ultrasound-targeted microbubble destruction [26]. Unfortunately, the nanoparticles for both of these studies were not well calibrated in size and neither paper discussed how the authors prevented the tendency of these nanoparticles to aggregate and interact with cell surfaces.

So far, only the delivery of cerium-oxide nanoparticles (average particle size 7 nm in diameter) to cardiac myocytes was confirmed after intravenous injection [27]. For normal conditions, the constraints for the delivery of nano-objects to cardiac cells remain unknown for particles ≥10 nm in size. Under some specific pathological conditions (i.e., infarction), all nanoparticles could reach cardiac myocytes owing to the disruption of blood capillaries [26,28]. Constraints on the delivery of nano-objects under specific pathological conditions remain to be elucidated.

Transmembrane transport of nano-objects

A number of studies with different particle types using different cell systems have confirmed that nano-objects can enter the cytosol and induce varying degrees of changes in cell-signaling pathways [29,30]. Collectively, these studies indicate that particle size, surface chemistry (coating) and, possibly, charge, govern translocation across cell membranes. In particular, the studies summarized by Mehta *et al.* [29] and those performed by Heckel *et al.* [31], using intravenous administration of 50–100 nm albumin-coated gold nanoparticles, demonstrated receptor-mediated endocytosis by caveolae. Vesicles containing the particles form invaginations of the plasmalemma coated with caveolin-1 protein. Similar transport of nano-objects mediated by an albumin receptor was suggested for heart myocytes [32].

Rejman *et al.* [33] reviewed a number of different endocytic pathways for internalization of a variety of substances, including clathrin-mediated endocytosis and caveolae-mediated endocytosis. They found, in nonphagocytic

cells, that internalization by clathrin-coated pits prevailed for nano-objects less than 200 nm in size; whereas, with increasing size up to 500 nm, caveolae became the predominant pathway. Recently, Qaddoumi *et al.* showed clathrin- and caveolin-independent uptake of 800 nm particles for epithelial cells using confocal microscopy [34], although this is somewhat suspect because confocal microscopy cannot produce reliable data for internalization of nanoparticles within 'flat' cultured cells because of signal input from out of focus light [35,36].

Electron microscopy (EM) data are much more convincing but somewhat controversial. Only particles ≤35 nm were shown to be translocated across the cell membrane [4,21,24,25,37]. However, these data also have some discrepancies. For example, Gupta and Gupta showed that polyethylene glycol-coated nanoparticles, but not protein-coated nanoparticles, could be internalized by human fibroblasts [4], whereas Ghitescu *et al.* showed, for the capillary endothelium, that gold complexes with polyethylene glycol produced a much lower intracellular labeling in comparison with that of gold coated with albumin [24].

Nonspecific translocation of nano-objects depends on their electrostatic interactions with negatively charged membrane domains governing the adsorption of the nanoparticles onto the cell membrane [38]. Anionic magnetic nanoparticles (~20 nm) were adsorbed by HeLa and RAW cells, whereas coating anionic particles with albumin strongly reduced both the nonspecific interactions with the plasma membrane and overall cell uptake [38]. Similar uptake of negatively charged gene carriers, copolymer/DNA nanospheres (~60 nm in diameter), was shown for muscle cells [5]. In this case, the delivery of nano-objects was confirmed by the expression of the corresponding proteins.

Recently, the existence of another nonspecific pathway for nanoparticles through the cell membrane, a circular energy-dominated pore, was predicted [39]. The mechanism of translocation involves the physical contact of the nano-object with peptide aggregates followed by the formation of the pore with an estimated critical radius of approximately 5 nm. The mechanism also predicts that particles ≥10 nm will be trapped and stay attached to the membrane. However, this mechanism has not yet been tested empirically.

Thus, theoretically, for ventricular myocytes, there are only three possible mechanisms for transport of nano-objects through the cell membrane: clathrin-mediated endocytosis, caveolae-mediated endocytosis and nonspecific penetration, the last of which does not involve total envelopment of the particle by the membrane [40]. Although the mechanisms of nano-object transport through the sarcolemma of cardiac myocytes remain to be clarified, some morphological data suggest that it is similar to that of the cells described earlier. Two types of caveolae, coated and uncoated (~100 and ~50 nm, correspondingly), that could be involved in transporting particles into cells have been demonstrated [41,42]. Meanwhile, only transport of nano-objects of approximately 3 nm in size has been shown in ventricular myocytes [16]. However, this was shown after only a 10 min co-incubation with intact myocytes, whereas similar experiments lasted for hours. This suggests that transport of larger nanoparticles into the sarcoplasm and associated mechanisms could be demonstrated in future experiments.

Some peptides can facilitate the permeation of nano-objects into the cells. In the past two decades, many cell-adhesion molecules (CAMs) have been discovered. CAMs are glycoproteins found on the cell surface that act as receptors for cell adhesion. CAMs can be divided into four classes: integrins, cadherins, selectins and the immunoglobulin superfamily [43]. Some CAMs are internalized into the cytoplasm during the recycling process by the formation of clathrin-coated pits and could be used for targeting nano-objects into specific cells. In recent years, peptides, peptidomimetics and proteins that bind to cell-adhesion receptors have been investigated for targeting drugs, particles and liposomes to specific cell-bearing cell-adhesion receptors (i.e., integrin and immunoglobulin superfamily) [6,43]. For example, some sequences participate in viral binding and infection, including:

- Five Arg–Gly–Asp (RGD motif) sequences per viral penton of human Ad2 or Ad12 bind to five $\alpha_v\beta_5$ integrins on the cell surface prior to internalization,
- Asp–Gly–Glu (DGE) from VP4 capsid protein that binds to $\alpha_2\beta_1$ integrin

Gly–Pro–Arg (GPR) and Leu–Asp–Val (LDV) sequences that are involved in binding between VP7 capsid protein and $\alpha_x\beta_2$, $\alpha_v\beta_3$ and $\alpha_4\beta_1$ integrins [43].

Figure 1. Cardiac myocyte.

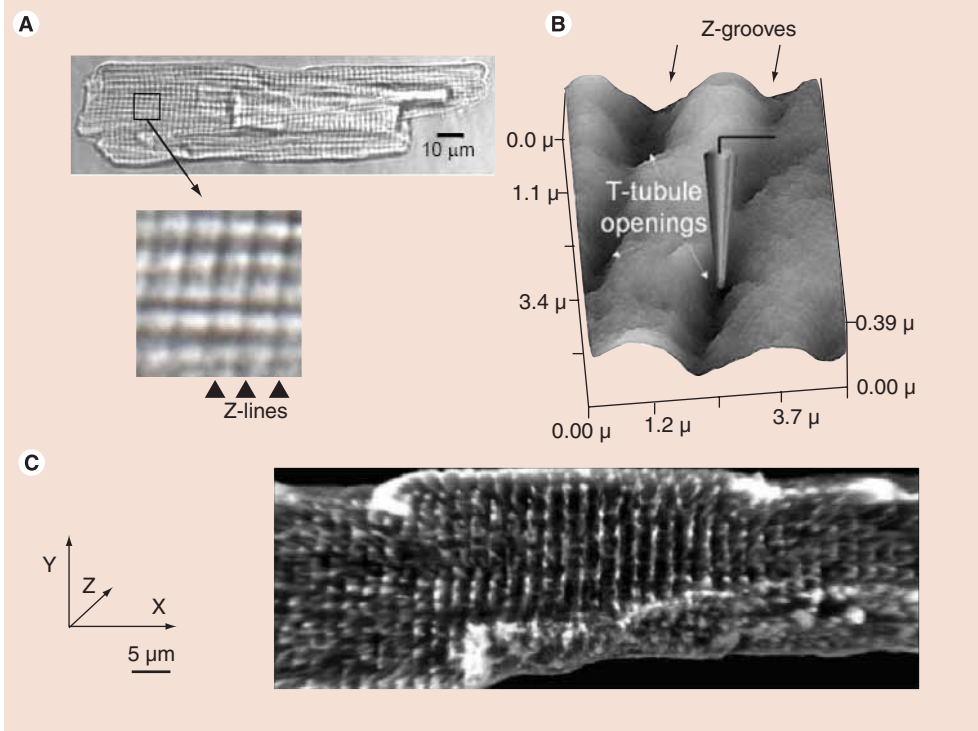

(A) Image of a ventricular cell in transmitted light. **(B)** Scanning ion-conductance micrograph (Adapted from [93]). **(C)** 3D confocal imaging of transverse-axial tubular system (TATS). Optical cut through the center of the cell. The TATS tubules are marked with di-8-ANEPPS.

Structure of a ventricular cell & cellular aqueous diffusion pathways for nano-objects

Ventricular cells are the biggest cardiac myocytes. These rod-shaped cells are approximately 100 µm in length and 20–30 µm thick (Figure 1). The characteristic cardiac stripes seen with light microscopy are a combination of extracellular Z-grooves (Figure 1B) and cytoskeletal Z lines. The sarcolemma has multiple invaginations, called T-tubules (Figure 1B), which are connected longitudinally into the transverse-axial tubular system (TATS). Figure 1C shows a complicated network of the TATS tubules penetrating the entire thickness of the ventricular myocyte. This helps spread the action potential and provides for diffusive access for ions, hormones and metabolic substrates throughout the entire thickness of the cardiac cell.

Z lines separate the myocytes into structurally similar sarcomeres. A longitudinal section presented in Figure 2 shows the main structures of the sarcomere: the myofibrillar and intermyofibrillar mitochondria, network and junctional SR and transverse tubules (T-tubules) of the TATS.

Thus, the aqueous pathways inside a ventricular myocytes can be divided into two groups:

- The extracellular tubules of the TATS [42,44–47]
- Sarcoplasmic aqueous-diffusion pathways [16].

The former is not a true intracellular system because of its multiple contacts with the extracellular space through T-tubules.

The diameters of the TATS tubules usually fall within the range of 200–360 nm [45,46]. However, they are filled with the glycocalyx [45,48,49], so the real clearance of the TATS pathway is approximately 10 nm [16].

The ultrastructure of cardiac myocytes suggests the existence of intracellular barriers significantly restricting the diffusion of nano-objects towards functionally important cellular compartments and structures, such as the nucleus, mitochondria and the space between the junctional sarcoplasmic reticulum (jSR) and the TATS tubules (so-called junctional cleft; JC) (Figure 3).

Which cellular domains are of primary interest for targeted delivery of nano-objects? Figure 3 shows the primary targets and possible barriers

Figure 2. Ultrastructure of rat ventricular cell.

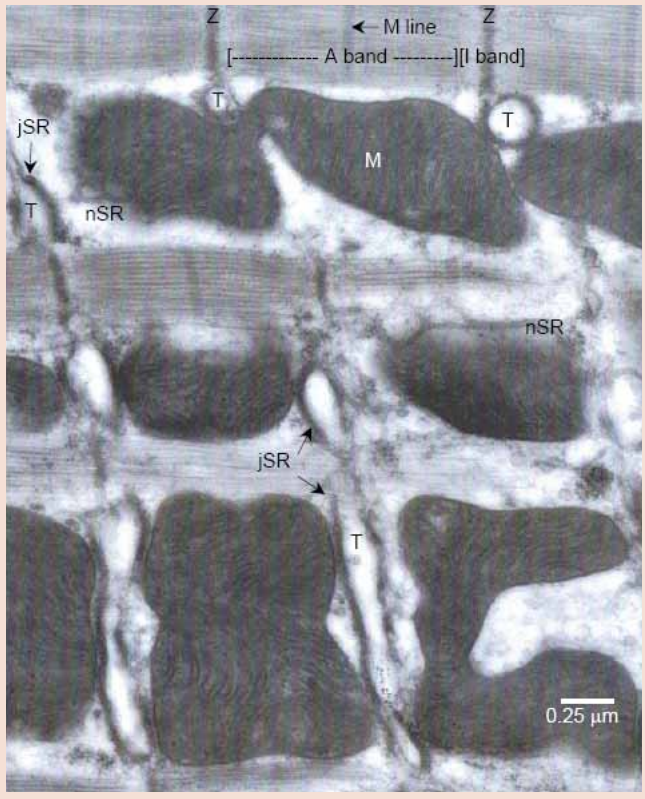

Electron micrograph; longitudinal ultrathin section, conventional fixation, polymerization in acrylic LR White. Oblique section shows localization of junctional SR (jSR) and network SR (nSR) in relation to T-tubules and mitochondria (M).
T: T-tubule of TATS; Z: Z line.
Adapted from [94].

and pathways for nano-objects within a cardiac myocyte. Targeting the nucleus and mitochondria is important because of their role in protein expression apoptosis and cell energetics. The TATS sarcolemma contains numerous transporting structures and receptors crucial for cardiac function. The structural organization of the space around the jSR is a matter of special interest because of its direct involvement in excitation–contraction coupling. This space includes a region between the intermyofibrillar mitochondrion (IMFM) and the T-tubule [16]. Electron micrographs (Figure 3B & C) show how tightly the intracellular microstructures are packed in this peri-T-tubule region [16,48,50,51]. However, under pathological conditions, cardiac cells undergo so-called ultrastructural remodeling, which increases the distance between the structures.

Heart failure-associated changes in ventricular cell ultrastructure

Heart failure is a syndrome with many different well-described causes, including myocardial infarction, pressure overload, volume overload, viral myocarditis, toxic cardiomyopathy and mutations in genes encoding for sarcomeric or cytoskeletal proteins [52]. Heart failure develops when the amount of blood pumped from the heart is inadequate to meet the metabolic demands of the body [52,53]. The symptoms include hypertrophy and abnormal excitation–contraction coupling and Ca^{2+} handling [52,54,55]. Heart hypertrophy is defined as enlarged heart size and muscle mass during dilated (congestive) cardiomyopathy. On the ultrastructural level, heart failure is characterized by lobulated nuclei, multiple intercalated discs, dilated T-tubules, reduction in the density of T-tubules and L-type Ca^{2+} channels, abnormal I bands, myofibrillar lysis, mitochondrial regressive changes (abnormally small mitochondria) and increased numbers of ribosomes [56–60]. Figure 4 shows a significant reduction in the density of intermyofibrillar mitochondria (IMFMs) and T-tubules and obvious mitochondrial regressive changes (abnormally small mitochondria; compare with Figure 2, in which the intermyofibrillar mitochondrion is as big as allowed by the space between the Z lines). The I bands are almost clear of electron-dense material. Electron micrographs are fundamentally shadowgrams, and the reduced density in the I bands results from less scattering material in the path of the electrons [61]. Under normal conditions, they are filled with glycogen particles and macromolecules [16,41].

These heart failure-related changes have to result in significant changes in the pathways for sarcoplasmic diffusion of nano-objects. The clearances of intracellular diffusion pathways for nano-objects under specific pathological conditions remain to be elucidated.

Novel methods for studying the delivery of nano-objects to intracellular sub-domains of cardiac myocytes

The actual space available for nano-objects is crucial to their engineering. Unfortunately, ultrastructural features of cardiac myocytes significantly complicate the localization of nano-objects within the cells using traditional fluorescent probes and confocal microscopy. Owing to input from out of focus light, nano-objects that are localized in TATS tubules (outside the cell) could

Figure 3. Intracellular targets for nano-objects in cardiac cell.

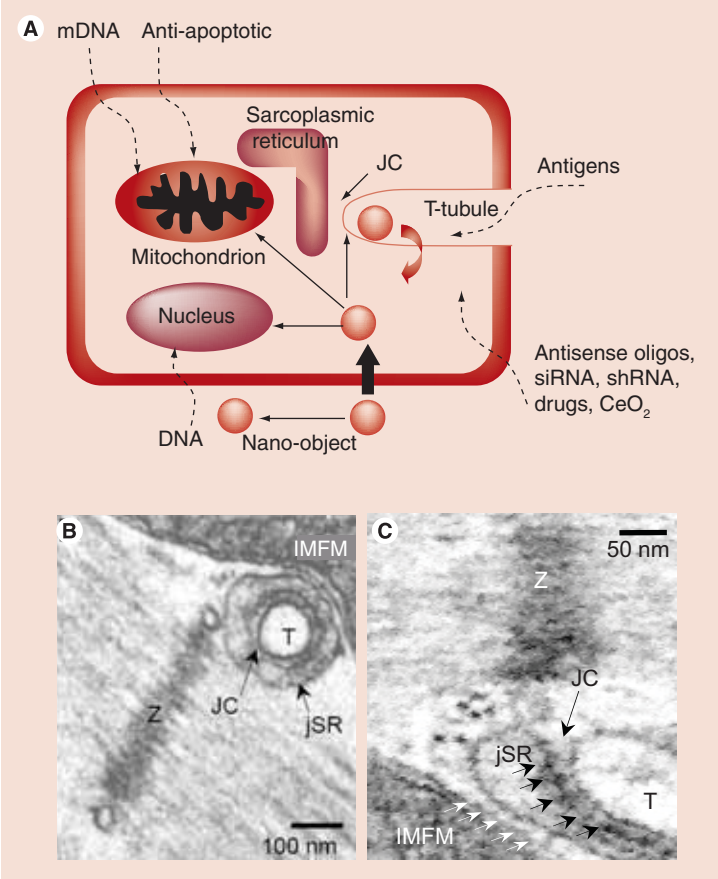

(A) Simplified schematic representation of intracellular targets for nano-objects in ventricular cell. **(B & C)** The electron micrographs show peri-T-tubule region in ventricular cell. Longitudinal ultrathin section, Epon embedding. Solid arrows show RyRs. White arrows show structures connecting the IMFM and jSR.
T-tubule, invagination in sarcolemma.
IMFM: Intermyofibrillar mitochondrion; JC: Junctional cleft; jSR: Junctional sarcoplasmic reticulum; mDNA: Mitochondrial DNA; RyRs: Ryanodine receptors; siRNA: Synthetic small interfering RNA; SR: Sarcoplasmic reticulum; T: T-tubule; Z: Z-line.
Adapted from [16].

be mistaken as being localized to the cytoplasm. EM provides the best possible measurements of distances within the cells. However, EM micrographs cannot be used directly for the measurement of nanodistances owing to fixation- and embedding-related changes. Recently, we showed that a cardiac cell loses up to 50% of its volume during the preparation for EM [16]. To avoid these problems, electrondense molecules (such as ferritin or imferon) and metallic nanoparticles have been used widely to measure intracellular distances in combination with EM. These techniques were pioneered by CM Feldherr in 1962 [62–66]. Unfortunately, his research focused only on the nucleus and mitochondria of non-muscle cells.

In 1971, Franzini-Armstrong used two electron-dense proteins, ferritin and imferon (iron-dextran complex), to find distances for the JC in skinned skeletal fibers [67]. These experiments surprisingly reveal that the larger-sized ferritin particles (~10 nm) could enter the JC, whereas smaller imferon particles (~3 nm) were not found within the JC. However, this can be explained by errors in the sizing of the molecules. Recently, London showed that the real diameter of imferon is 5–10 nm, previously significantly underestimated [68]. Other recent measurements of the mitochondrial outer-membrane pores (VDAC) suggested that the size of ferritin must have been overestimated. The VDAC pore is ≤3 nm in diameter, and this is the only gate between the cytoplasm and the mitochondrial intermembrane space [69]. In 1962, Feldherr showed that, after cell injection, ferritin was localized between the outer and inner mitochondrial membranes [70]. A similar distribution of ferritin could be seen in liver cells [71] and in skinned skeletal fibers [67]. Thus, ferritin must be smaller than 3 nm to be able to fit through VDACs. Although the ferritin molecule iron core is approximately 2.0 nm in size [71], the real diameter is larger, owing to the dextran shell, which should add at least 1 nm to the diameter of the ferritin-iron core. Thus, the experiments by Franzini-Armstrong really showed that the JC of skeletal muscles is only accessible to particles ≤3 nm in size, when using the corrected diameters [67]. The data for ventricular myocytes should be similar.

Recently, we developed a much more precise method to measure intracellular-diffusion pathways and to visualize single gold nanoparticles within ventricular cells [16,72]. This method is shown in Figure 5. We attached isolated cardiac cells to coverslips, then added polyvinylpyrrolidone (PVP)-coated gold nanoparticles to the bath solution for 10 min. The cells were then fixed in 6% glutaraldehyde, embedded in water-soluble resin and ultrathin sections were prepared. We used intact and permeabilized cells. A high concentration of glutaraldehyde enabled us to fix nanoparticles within the cell. To visualize the particles, we used silver enhancement. Water-soluble resin enabled silver ions to penetrate through the body of the ultrathin section and to mark even the smallest gold nanoparticles for EM. Therefore, our electron micrographs actually show the distribution of the silver grains; note that the closer the particle was to the center of section, the smaller the grain (Figure 5).

Figure 4. Ultrastructure of ventricular cell from rat suffering from heart failure.

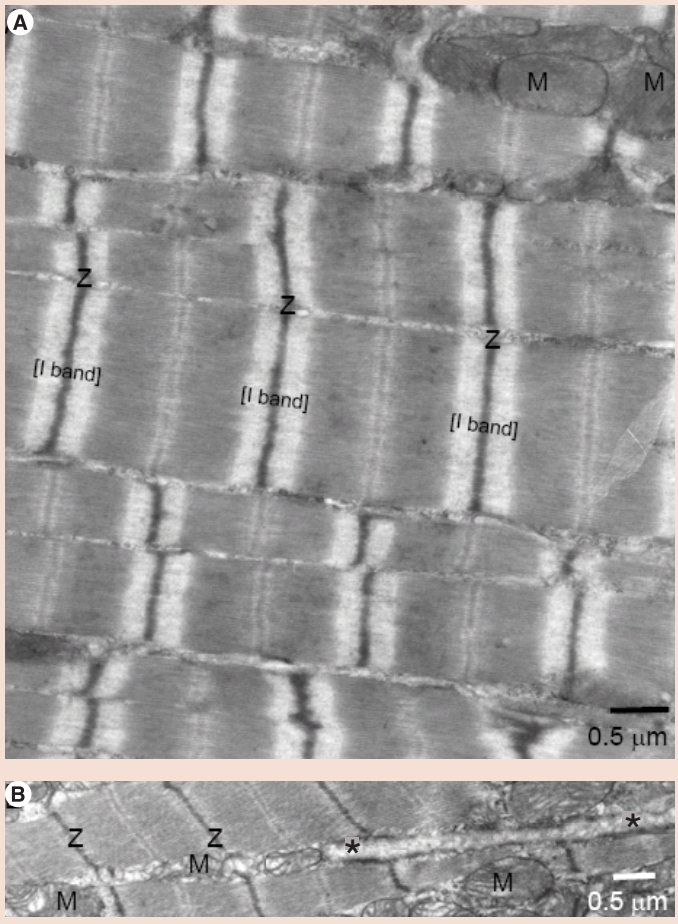

Heart failure was induced with isoproterenol (third week; 0.3 mg/kg injections). Compare it with **Figure 2**. Note mitochondrial regressive changes **(A & B)** and abnormal I bands **(A)**. **(B)** The marked structure (*) is a dilated longitudinal tubule. Left ventricle; conventional microwave fixation.
M: Mitochondrion; Z: Z line.

Another method for studying pathways for nano-objects within cardiac myocytes is the expression of biological markers, which could be considered as nano-objects owing to their size. We used GFP (enhanced) [72], which is a 4.2 nm long cylinder with a cylindrical diameter of 2.4 nm [73]. This method, however, has some restrictions. Expression of any protein, even a nonfunctional one, such as enhanced GFP, can result in heart failure [74], and protein synthesis must be inhibited with doxycycline [75]. This, however, reduces the synthesis of other cell proteins as well.

Diffusion of nano-objects within ventricular cells under quasi-physiological conditions

We used both novel methods described here for probing the diffusion pathways under quasi-physiological conditions [16,72]. TATS is a part of an extracellular pathway for nano-objects towards the sarcolemma of ventricular myocytes. Although TATS tubules have a diameter up to 300 nm, the diffusion of nano-objects in the TATS tubules could be decreased by the glycocalyx [49]. The addition of calibrated gold nanoparticles with the smallest size in the groups being 3, 6, 11, 16 and 21 nm to intact ventricular myocytes showed that TATS tubules are available only for nano-objects ≤11 nm (Figure 6). Note that all the particles are of equal size before silver enhancement. As noted earlier, the apparent size of the smaller particles on the micrographs results from a deeper location within the ultrathin section and their relative inaccessibility for silver enhancement.

Only 3 nm particles were found within the cytoplasm [16]. Theoretically, the 3-nm particles added to intact myocytes could enter the cytoplasm by endocytosis or through a nonspecific pathway. Unfortunately, the experimental conditions of cell fixation and resin polymerization did not enable the visualization of membranes of endocytotic vesicles and, thus, this mechanism of transport remains to be confirmed. The penetration of the particles through the sarcolemma was Ca^{2+} dependent. Contraction inhibited the transportation of the nanoparticles significantly. This suggests that the delivery of nano-objects to the cytoplasm could be facilitated significantly under pathological conditions when the contractility of the cells is reduced.

To check the availability of the intracellular subdomains for nano-objects *in vivo*, we expressed GFP in ventricular cells [72]. The expressed GFP was seen readily within the nucleus, along Z lines, but not in the mitochondria (Figure 7). This was somewhat unexpected to us.

A mitochondrion has two membranes. Under normal conditions, the biggest channel in the outer mitochondrial membrane is a voltage-dependent anion channel (also known as VDAC or porin) [76]. The diameter of the VDAC pore in non-muscle cells was shown to be approximately 3 nm [69,77]. Thus, GFP should be able to permeate the VDAC (at pH7.2; -5.6; protein calculator v3.3), but it does not. This suggests that under normal conditions the VDAC pore might be inaccessible for nano-objects owing to

the existence of unknown barriers in the way of the particles to mitochondrial intermembrane space *in vivo*.

Diffusion of nano-objects within ventricular cells under conditions simulating heart failure-related ultrastructural remodeling

During heart failure, tubules of TATS undergo significant dilation. We mimicked these ultrastructural changes by exposing the cells to sialidase neuraminidase, which unseals the tubules [78]. This pretreatment made the TATS tubules much more accessible for nano-objects. The graph presented in Figure 6C shows the density data versus particle size for contracting ventricular myocytes before and after the neuraminidase treatment.

Isolated cardiac mitochondria can simulate one of the aspects of ultrastructural remodeling during heart failure (see earlier). We used 3 and 6 nm PVP-coated gold particles to determine whether nano-objects can diffuse into the mitochondria when pathways to the mitochondrial outer membrane are free [72]. To find these nanoparticles within the mitochondria, we put isolated cardiac mitochondria on a dry coverslip and then washed off unbound mitochondria. To prepare them for EM and visualize the nanoparticles, we used the method described earlier (Figure 5).

Figure 5. Localization of PVP-coated gold nanoparticles within cardiac cells.

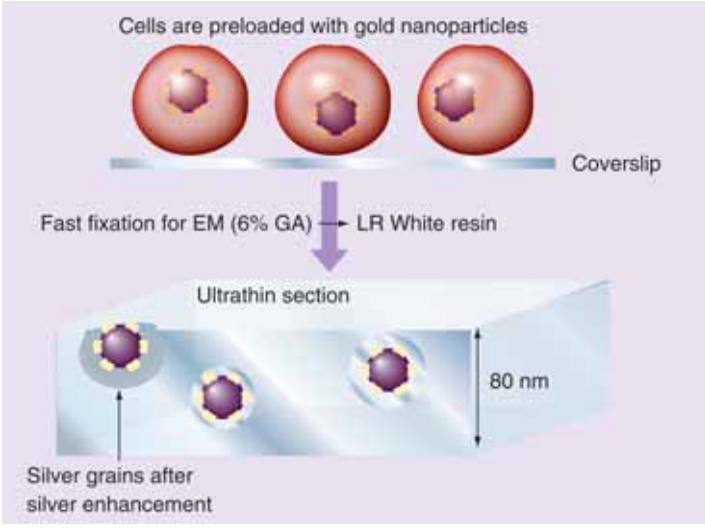

Simplified schematic representation of a method for localization of PVP-coated gold nanoparticles embedded in water-soluble resin for silver enhancement.
EM: Electron microscopy; PVP: Polyvinylpyrrolidone.

The 3-nm particles were found within the mitochondria (Figure 8). Their density was similar to the density of the particles in the experimental solution and their entry was prevented by known inhibitors of VDAC, Koenig's polyanion (KPA) and 2,2'-(1,2-ethenediyl)bis(5-isothiocyanatobenzenesulfonic acid) (DIDS)[72]. The 6 nm particles did not enter the mitochondria. However, they did enter the mitochondria after permeabilization of mitochondrial membranes with alamethicin [72].

Thus, during heart failure, the mitochondria could be accessible at least for particles approximately 3 nm in size. We checked this hypothesis in permeabilized ventricular cells. For these experiments, we used a similar protocol: nanoparticles were added to saponin-permeabilized ventricular cells for 20 min and then fixed for EM.

The 3-nm particles were found within the mitochondria and the nucleus (Figure 9A). However, there is a big difference in the densities of particles found within these and the isolated mitochondria. Although in both experiments the mitochondrial outer membranes were not damaged, isolated cardiac mitochondria had approximately 20 times the density as the mitochondria of permeabilized myocytes [72]. The velocity of nanoparticle diffusion within myocytes (0.5 μm/s) suggests an even distribution of nanoparticles within mitochondria for both cases [79]. The data confirmed our hypothesis that, *in vivo*, the entrance to the VDAC pore could be protected by cytosolic structures. The VDAC pore entrance *in vivo* could be covered by huge hexokinases II [80,81], which have to be lost during the preparation of isolated cardiac mitochondria.

The 6 nm particles entered the cells and were located mainly along the Z lines (Figure 9B). However, these nanoparticles did not enter the mitochondria, JC, mitochondrion–jSR junction, intermitochondrial junctions or the nucleus. Figure 9C shows that, although some particles are located in close proximity to the nucleus, none have entered it. Earlier, Bustamante *et al.* showed that FITC-labeled dendrimers of 5.4 nm but not 8 nm diffused freely into the nucleus [82] . Comparison of the data with our data mentioned earlier suggests that the nuclear-pore complex is available for free diffusion of nano-objects ≤5.5 nm in size.

The particles ≥11 nm in our experiments did not enter the permeabilized ventricular myocytes (Figure 9D) [16]. However, partial destruction of the cytoskeleton with cytochalasin D increases permeation of nano-objects into the cells significantly (Figure 9E & F).

Figure 6. Distribution of gold nanoparticles in intact contracting ventricular myocytes.

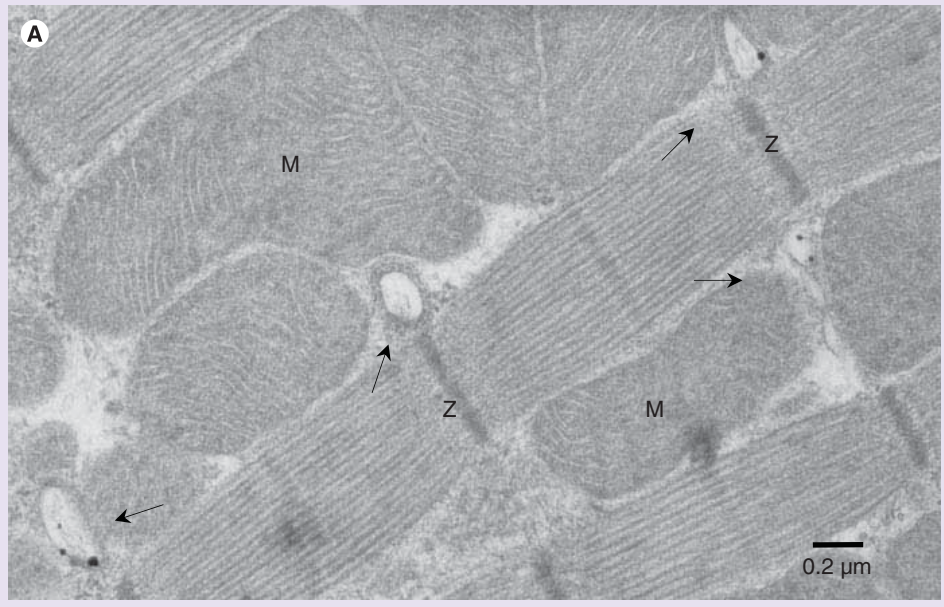

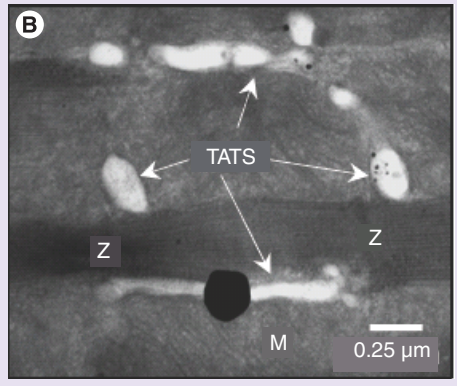

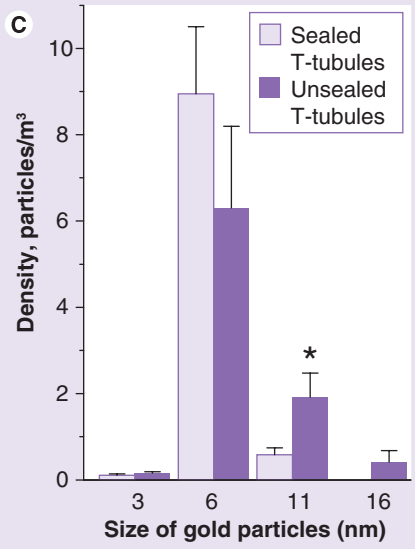

(A,B) Representative electron micrographs show the distribution of 6-nm particles in T-tubules **(A)** and longitudinal tubules of TATS **(B)**. Note that all particles are of equal size before silver enhancement. However, the apparent size of the smaller particles on the micrographs results from a deeper location within the ultrathin section and their relative inaccessibility for silver enhancement. M: mitochondrion; TATS: transverse-axial tubular system; Z: Z line; black arrows, T-tubules. **(C)** The graphs represent the density of nanoparticles in the ventricular cells before (grey) and after (dark grey) 4 hours of pretreatment with 0.3 u/ml neuraminidase (i.e., when T-tubules are partially unsealed). Data were expressed as mean ± SE; n = 23 - 190; * - data are statistically different from the corresponding control ($P < 0.01$); $[Ca^{2+}] = 5$ mM. Adapted from [16].

First successes in cardiac nanomedicine

To exert their therapeutic action, many pharmacological agents and large regulatory molecules (i.e., antiapoptotic drugs, enzymes, siRNA and shRNA) have to be delivered intracellularly (Figure 3). Precise delivery of different biologically active molecules to cellular sub-domains of failing cardiac myocytes can benefit the entire heart function.

Figure 7. GFP fluorescence visualizes intracellular aqueous diffusion pathways.

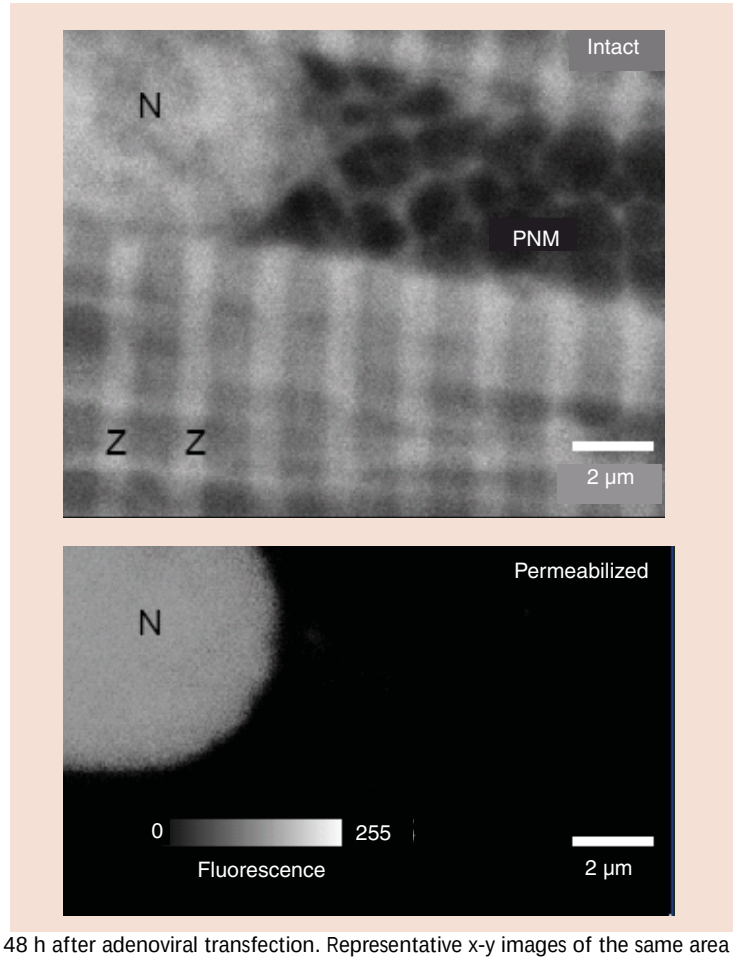

48 h after adenoviral transfection. Representative x-y images of the same area of ventricular cells before and after saponin permeabilization. [Ca^{2+}] = 90 nM. GFP: Green fluorescent protein; N: Nucleus; PNM: Perinuclear mitochondria; Z: Z lines.
Adapted from [72].

Figure 8. 3- but not 6-nm particles enter isolated cardiac mitochondria.

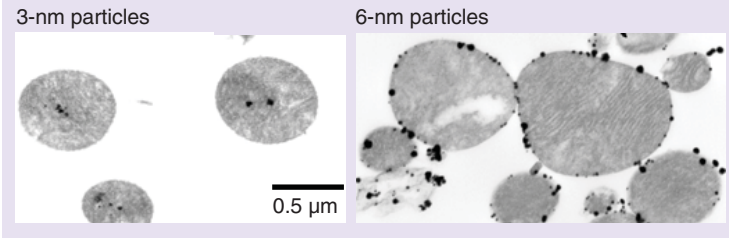

Ultrathin electron micrographs; LR White resin; [Ca^{2+}] = 90 nM; [Na^{+}] = 10 mM.
Adapted from [72].

Recently, the first papers describing real improvements from nanotherapy were published. First, Richard Lee's laboratory showed that 5–10 nm self-assembling peptide nanofibers create nanofiber microenvironments for endothelial cells in the myocardium and promote vascular cell recruitment [28]. This approach might enable injectable tissue regeneration strategies. Then, Joseph Metzger's laboratory showed that cardiac performance *in vitro* and *in vivo* is enhanced when a single histidine residue present in the fetal cardiac Troponin I isoform is substituted into the adult cardiac Troponin I isoform at codon 164 [83]. The authors observed most marked effects under the acute challenges of acidosis, hypoxia, ischemia and ischemia–reperfusion, in chronic heart failure in transgenic mice and in myocytes from failing human hearts. In the isolated heart, histidine-modified Troponin I improved systolic and diastolic functions and mitigated reperfusion-associated ventricular arrhythmias. This research opens new avenues for improving myocardial performance in the ischemic and failing heart.

Recently, Vladimir Torchilin's laboratory reported the successful delivery of ATP-loaded immunoliposomes specific for cardiac myosin to cardiac myocytes of isolated rat hearts [84]. This significantly improved heart contractility after global ischemia . Finally, Kolattukudy's laboratory demonstrated cardioprotective effects of cerium oxide (CeO_2) nanoparticles in cardiomyopathy [27]. The nanoparticle treatment attenuated progressive cardiac dysfunction and remodeling in a murine model of ischemic cardiomyopathy. The authors attributed this beneficial effect of CeO_2 nanoparticles to their autoregenerative antioxidant properties inhibiting myocardial oxidative stress, ER stress and inflammatory processes.

Conclusion

Nanotechnology is expected to be important in individualized gene therapy of heart failure; however, it will not be as effective as it promises unless we can target therapy to precisely the right location. Understanding what pathways are available and knowing the constraints of these pathways for nanoparticles is crucial to advancing the use of nano-objects for biological and medical applications.

This analysis of the literature shows that, under normal conditions, the delivery of nanoparticles to the sub-domains of cardiac cells is restricted by multiple factors, including the glycocalyx within TATS, the cytoskeleton, the size of the nuclear pore and cytosolic structures. In addition, the

Figure 9. Distribution of gold nanoparticles in permeabilized ventricular myocytes.

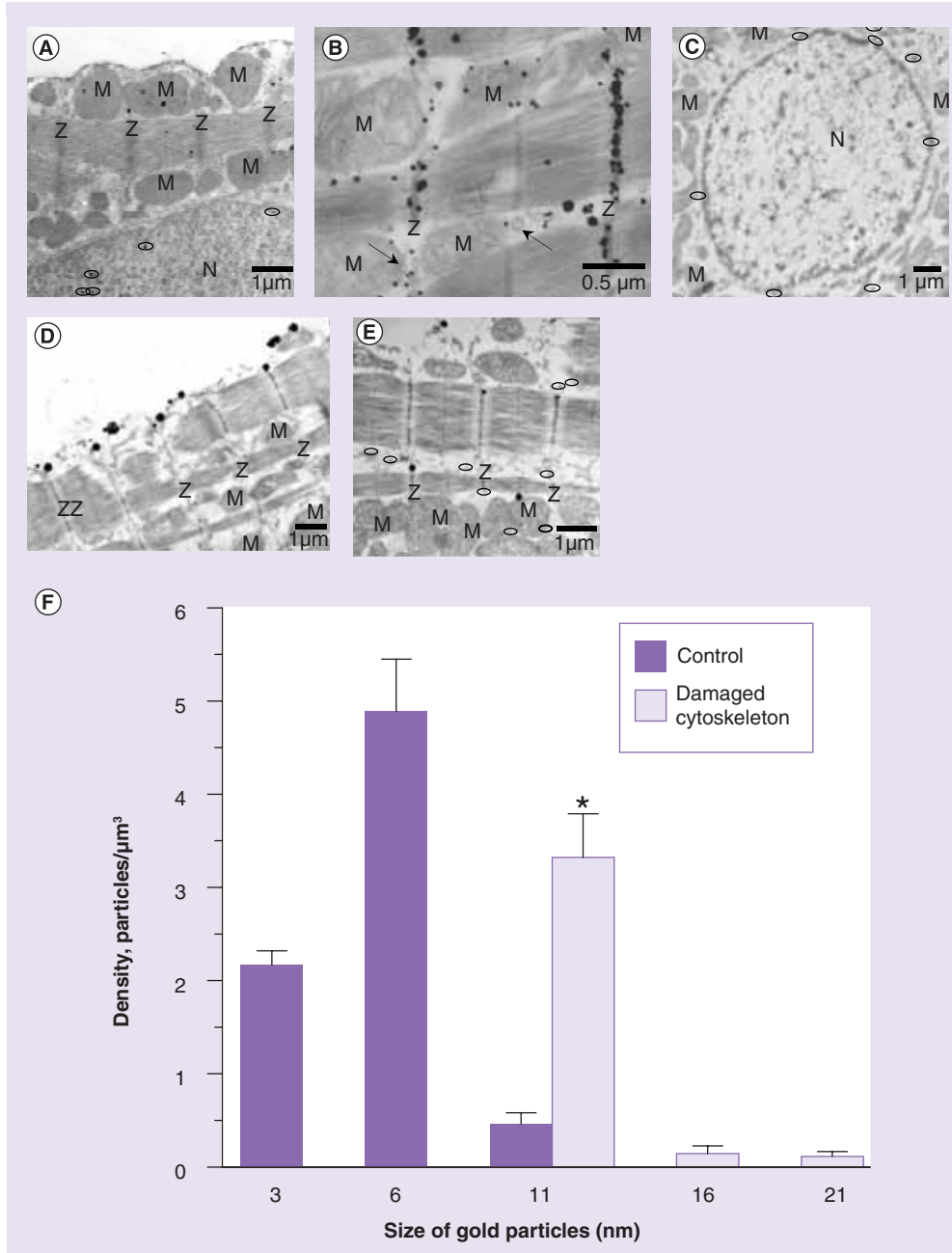

*Data are statistically different from the corresponding control ($p < 0.001$). **(A–D)** Representative electron micrographs show the distribution of 3 **(A)**, 6 **(B,C)** and 11 **(D)** nm particles within ventricular cells under control conditions. **(E)** Distribution of 11 nm particles in the ventricular cells after partial destruction of cytoskeleton by cytochalasin D. Arrows show the location of T-tubules. Ovals mark particles located deeper in the section and found with digitally enhanced contrast. **(F)** Graphs representing the density of nanoparticles in the ventricular cells before (gray) and after (dark gray) 20 min of pretreatment with 40 µM cytochalasin D. n = 26–308.

M: Mitochondrion; N: Nucleus; Z: Z line.

Adapted from [16].

contraction of the cells impedes nanoparticles from entering the cells. Cytosolic diffusion in ventricular cells is highly restricted for particles more than 11 nm in size. The JC and mitochondrial intermembrane space are almost inaccessible for particles with physical sizes ≥3 nm. The nuclear-pore complex is accessible for nano-objects less than 6 nm. However, after heart failure-induced structural remodeling, the accessibility of cytoplasm and mitochondria for nano-objects could be increased significantly in failing ventricular cells owing to the dilation of TATS tubules, the availability of the VDAC pore and a possible increase in transportation through the sarcolemma of noncontracting cells. This increases the probability for the delivery of drugs and genes to failing cells. Therefore, nanomedicine could be highly effective in slowing down the development of heart failure, and perhaps even in curing it.

Future perspective

Mapping the pathways for nano-objects will: enhance the general scientific and technological understanding of potential biotechnology applications; facilitate the use of nano-objects in biological research, medical diagnostics and therapy; and improve mathematical modeling (i.e., understanding) of processes within cellular compartments and structures. The questions remaining to be answered are:

- What size of nano-objects can reach which cellular sub-domains in failing hearts?
- What are the mechanisms for their permeation through the sarcolemma?
- How can the delivery of nano-objects to cardiomyocytes be improved?
- How can nano-objects be delivered to the mitochondrial matrix?

First, the major task is to determine the size constraints of the pathways for delivery of nano-objects to the cellular sub-domains of ventricular and atrial myocytes in failing hearts. This could be done during the next 5 years with our novel method described here [16,72]. So far, only this method enables the precise localization of calibrated nano-objects within the cytoplasm of heart tissue. Meanwhile, multiple fluorescent markers could be used to study the *in vivo* delivery of nano-objects to nuclei or mitochondria in cardiac myocytes.

Second, several mechanisms of membrane translocation for ventricular myocytes have been suggested in this review but have yet to be investigated fully. Methods for studying the mechanisms of endocytosis include:

- Inhibition of the energy metabolism with ATP depletion of both oxidative and glycolytic pathways;
- Inhibition of clathrin assembly with potassium depletion;
- Pharmacological inhibition of clathrin endocytosis or inhibition through overexpression of p50/dynamitin (a dynamin inhibitory peptide);
- Expression of epidermal growth factor receptor pathway substrate clone 15 (Eps15) or dominant-negative dynamin mutants for the inhibition of clathrin endocytosis [85–90].

Third, the search for targeted drug- or gene-delivery systems for the heart needs to be accelerated. This includes the use of synthetic peptides to enhance the transport of nano-objects to cardiac intracellular structures (i.e., to develop a novel delivery system for ventricular myocytes). The way to improve the delivery of nanoparticles to the cytosol of ventricular myocytes is to use different peptide–BSA or peptide–PEG conjugates for coating the nanoparticles and to develop more effective nanocarriers with novel properties (i.e., geometrical and physicochemical) [6,11,84].

Fourth, one of the most important problems for contemporary bioresearch and therapy is the delivery of nano-objects to the mitochondrial matrix (reviewed in [15]). The double mitochondrial membrane is a serious barrier for nano-objects. One strategy for their delivery is the use of mitochondrial fusion mechanisms, that is, the creation of double-membrane liposomes carrying specific mitochondrial fusion proteins [91,92].

Acknowledgements

We thank Dr V Salnikov and Dr A Ziman (Medical Biotechnology Center, University of Maryland Biotechnology Institute, Baltimore, MD) for their help in the preparation of electron and confocal microscopy images.

Financial & competing interests disclosure

The author has no relevant affiliations or financial involvement with any organization or entity with a financial interest in or financial conflict with the subject matter or materials discussed in the manuscript. This includes employment, consultancies, honoraria, stock ownership or options, expert testimony, grants or patents received or pending or royalties.

No writing assistance was utilized in the production of this manuscript.

Executive summary

Nano-objects in biomedical research

- Nano-objects with important analytical applications.
- The pathway for nano-objects to target an intracellular sub-domain.

Constraints in delivery of nano-objects from capillary to cardiac cells

- The ability of the nano-objects to penetrate through the barrier of the continuous microvascular endothelium.
- Size constraints for delivery of nano-objects to heart cells.

Transmembrane transport of nano-objects

- Endocytic pathways for internalization of nano-objects.
- Nonspecific translocation of nano-objects.
- Three possible mechanisms for transport of nano-objects through the membrane of cardiomyocytes.
- Facilitation of the targeted delivery of nano-objects to cellular sub-domains.

Structure of a ventricular cell and cellular aqueous diffusion pathways for nano-objects

- The aqueous pathways inside a ventricular myocytes can be divided into two groups.
- Intracellular barriers for diffusion of nano-objects.
- Cardiomyocyte domains, which are of primary interest for targeted delivery of nano-objects.

Changes in ventricular cell ultrastructure associated with heart failure

- The symptoms for heart failure.
- The accessibility of cytoplasm and mitochondria for nano-objects may be significantly increased in failing ventricular cells.

Novel methods for studying the delivery of nano-objects to intracellular sub-domains of cardiac myocytes

- Problems with localization of nano-objects within cardiac myocytes.
- Polyvinylpyrrolidone (PVP)-coated gold nanoparticles embedded in water-soluble resin for silver enhancement.
- Expression of fluorescent protein markers.

Diffusion of nano-objects within ventricular cells under quasi-physiological conditions.

- Availability of transverse-axial tubular system for nano-objects.
- Nano-objects cannot diffuse into the mitochondrial intermembrane space.

Diffusion of nano-objects within ventricular cells under conditions simulating heart failure-related ultrastructural remodeling

- Availability of mitochondrial intermembrane space for diffusion of nano-objects.
- Specific distribution of nano-objects ≥6 nm along Z lines.
- Role of the cytoskeleton in the restriction of free diffusion of nano-objects in cytoplasm.

First successes in cardiac nanomedicine

- Nanofiber microenvironments in the myocardium.
- Cardioprotective effects of cerium oxide nanoparticles.
- Tuning cardiac performance in ischemic heart disease.

Bibliography

Papers of special note have been highlighted as either of interest (•) or of considerable interest (••) to readers.

1. Åkerman ME, Chan WC, Laakkonen P *et al.*: Nanocrystal targeting *in vivo*. *Proc. Natl Acad. Sci. USA* 99, 12617–12621 (2002).
2. Kwon GS: Polymeric micelles for delivery of poorly water-soluble compounds. *Crit. Rev. Ther. Drug Carrier Syst.* 20, 357–403 (2003).
3. Penn SG, He L, Natan MJ: Nanoparticles for bioanalysis. *Curr. Opin. Chem. Biol.* 7, 609–615 (2003).
4. Gupta AK, Gupta M: Synthesis and surface engineering of iron oxide nanoparticles for biomedical applications. *Biomaterials* 26, 3995–4021 (2005).
5. Pitard B, Bello-Roufai M, Lambert O *et al.*: Negatively charged self-assembling DNA/poloxamine nanospheres for *in vivo* gene transfer. *Nucleic Acids Res.* 32, e159–e167 (2004).
6. Tkachenko AG, Xie H, Liu Y *et al.*: Cellular trajectories of peptide-modified gold particle complexes: comparison of nuclear localization signals and peptide transduction domains. *Bioconjug. Chem.* 15, 482–490 (2004).
7. Bibby DC, Talmadge JE, Dalal MK *et al.*: Pharmacokinetics and biodistribution of RGD-targeted doxorubicin-loaded nanoparticles in tumor-bearing mice. *Int. J. Pharm.* 293, 281–290 (2005).
8. Kohli P, Martin CR: Smart nanotubes for biotechnology. *Curr. Pharm. Biotechnol.* 6, 35–47 (2005).
9. Melton L: Imaging: the big picture. *Nature* 437, 775–779 (2005).
10. Kong DF, Goldschmidt-Clermont PJ: Tiny solutions for giant cardiac problems. *Trends Cardiovasc. Med.* 15, 207–211 (2005).
11. Nan A, Ghandehari H, Hebert C *et al.*: Water-soluble polymers for targeted drug delivery to human squamous carcinoma of head and neck. *J. Drug Target.* 13, 189–197 (2005).
12. Brewster LP, Brey EM, Greisler HP: Cardiovascular gene delivery: the good road is awaiting. *Adv. Drug Deliv. Rev.* 58, 604–629 (2006).

13. Park TG, Jeong JH, Kim SW: Current status of polymeric gene delivery systems. *Adv. Drug Deliv. Rev.* 58, 467–486 (2006).
14. Torchilin VP: Recent approaches to intracellular delivery of drugs and DNA and organelle targeting. *Annu. Rev. Biomed. Eng.* 8, 343–375 (2006).
•• Best review of nanomedicine research.
15. Weissig V, Boddapati SV, Jabr L, D'Souza GG: Mitochondria-specific nanotechnology. *Nanomedicine* 2, 275–285 (2007).
16. Parfenov AS, Salnikov V, Lederer WJ, Lukyanenko V: Aqueous diffusion pathways as a part of the ventricular cell ultrastructure. *Biophys. J.* 90, 1107–1119 (2006).
• First nanobiological paper describing intracellular barriers within cardiac myocytes.
17. Fortina P, Kricka LJ, Surrey S, Grodzinski P: Nanobiotechnology: the promise and reality of new approaches to molecular recognition. *Trends Biotechnol.* 23, 168–173 (2005).
18. Tallini YN, Ohkura M, Choi BR *et al.*: Imaging cellular signals in the heart *in vivo*: cardiac expression of the high-signal Ca2+ indicator GCaMP2. *Proc. Natl Acad. Sci. USA* 103, 4753–4758 (2006).
19. Majoros IJ, Myc A, Thomas T *et al.*: PAMAM dendrimer-based multifunctional conjugate for cancer therapy: synthesis, characterization and functionality. *Biomacromolecules* 7, 572–579 (2006).
20. Kreiss P, Cameron B, Rangara R *et al.*: Plasmid DNA size does not affect the physicochemical properties of lipoplexes but modulates gene transfer efficiency. *Nucleic Acids Res.* 27, 3792–3798 (1999).
21. Riviere C, Boudghene FP, Gazeau F *et al.*: Iron oxide nanoparticle-labeled rat smooth muscle cells: cardiac MR imaging for cell graft monitoring and quantitation. *Radiology* 235, 959–967 (2005).
22. Rosi NL, Giljohann DA, Thaxton CS *et al.*: Oligonucleotide-modified gold nanoparticles for intracellular gene regulation. *Science* 312, 1027–1030 (2006).
23. Sebestyen MG, Budker VG, Budker T *et al.*: Mechanism of plasmid delivery by hydrodynamic tail vein injection. I. Hepatocyte uptake of various molecules. *J. Gene Med.* 8, 852–873 (2006).
24. Ghitescu L, Fixman A, Simionescu M, Simionescu N: Specific binding sites for albumin restricted to plasmalemmal vesicles of continuous capillary endothelium: receptor-mediated transcytosis. *J. Cell Biol.* 102, 1304–1311 (1986).
25. Predescu D, Palade GE: Plasmalemmal vesicles represent the large pore system of continuous microvascular endothelium. *Am. J. Physiol.* 265, H725–H733 (1993).
26. Vancraeynest D, Havaux X, Pouleur AC *et al.*: Myocardial delivery of colloid nanoparticles using ultrasound-targeted microbubble destruction. *Eur. Heart J.* 27, 237–245 (2006).
27. Niu J, Azfer A, Rogers LM *et al.*: Cardioprotective effects of cerium oxide nanoparticles in a transgenic murine model of cardiomyopathy. *Cardiovasc Res.* 273, 549–559 (2007).
• First nanomedical paper relevant to real therapeutic effect of nanoparticles delivered into cardiac cells.
28. Davis ME, Motion JP, Narmoneva DA *et al.*: Injectable self-assembling peptide nanofibers create intramyocardial microenvironments for endothelial cells. *Circulation* 111(4), 442–450 (2005).
•• Nanoparticles create nanofiber microenvironments in the myocardium and promote vascular cell recruitment. This approach may enable injectable tissue regeneration strategies.
29. Mehta D, Bhattacharya J, Matthay MA, Malik AB: Integrated control of lung fluid balance. *Am. J. Physiol. Lung Cell Mol. Physiol.* 287, L1081–L1090 (2004).
30. Oberdörster G, Oberdörster E, Oberdörster J: Nanotoxicology: an emerging discipline evolving from studies of ultrafine particles. *Environ. Health Perspect.* 113, 823–839 (2005).
31. Heckel K, Kiefmann R, Dorger M *et al.*: Colloidal gold particles as a new *in vivo* marker of early acute lung injury. *Am. J. Physiol. Lung Cell Mol. Physiol.* 287, L867–L878 (2004).
32. Hutter JF, Piper HM, Spieckermann PG: Myocardial fatty acid oxidation: evidence for an albumin-receptor-mediated membrane transfer of fatty acids. *Basic Res. Cardiol.* 79, 274–282 (1984).
33. Rejman J, Oberle V, Zuhorn IS, Hoekstra D: Size-dependent internalization of particles via the pathways of clathrin- and caveolae-mediated endocytosis. *Biochem. J.* 377, 159–169 (2004).
34. Qaddoumi MG, Gukasyan HJ, Davda J *et al.*: Clathrin and caveolin-1 expression in primary pigmented rabbit conjunctival epithelial cells: role in PLGA nanoparticle endocytosis. *Mol. Vis.* 9, 559–568 (2003).
35. Pratusevich VR, Balke CW: Factors shaping the confocal image of the calcium spark in cardiac muscle cells. *Biophys. J.* 71, 2942–2957 (1996).
36. Sedarat F, Lin E, Moore ED, Tibbits GF: Deconvolution of confocal images of dihydropyridine and ryanodine receptors in developing cardiomyocytes. *J. Appl. Physiol.* 97, 1098–1103 (2004).
37. Bruns RR, Palade GE.: Studies on blood capillaries. II. Transport of ferritin molecules across the wall of muscle capillaries. *J. Cell Biol.* 37, 277–299 (1968).
38. Wilhelm C, Billotey C, Roger J *et al.*: Intracellular uptake of anionic superparamagnetic nanoparticles as a function of their surface coating. *Biomaterials* 24, 1001–1011 (2003).
39. Livadaru L, Kovalenko A: Fundamental mechanism of translocation across liquidlike membranes: toward control over nanoparticle behavior. *Nano Lett.* 6, 78–83 (2006).
40. Page E, Goings, GE Upshaw-Earley J, Hanck DA: Endocytosis and uptake of lucifer yellow by cultured atrial myocytes and isolated intact atria from adult rats. Regulation and subcellular localization. *Circ. Res.* 75, 335–346 (1994).
41. Fawcett DW, McNutt NS: The ultrastructure of the cat myocardium. I. Ventricular papillary muscle. *J. Cell Biol.* 42, 1–45 (1969).
•• One of the two best papers about ultrastructure of cardiac myocyte.
42. McNutt NS, Fawcett DW: The ultrastructure of the cat myocardium. II. Atrial muscle. *J. Cell Biol.* 42, 46–67 (1969).
• One of the two best papers about ultrastructure of cardiac myocyte.
43. Dunehoo AL, Anderson M, Majumdar S *et al.*: Cell adhesion molecules for targeted drug delivery. *J. Pharm. Sci.* 95, 1856–1872 (2006).
44. Leeson TS: T-tubules, couplings and myofibrillar arrangements in rat atrial myocardium. *Acta. Anat. (Basel)* 108, 374–388 (1980).
45. Forbes MS, van Neil EE: Membrane systems of guinea pig myocardium: ultrastructure and morphometric studies. *Anat. Rec.* 222, 362–379 (1988).
46. Ogata T, Yamasaki Y: Ultra-high resolution scanning electron microscopic studies on the sarcoplasmic reticulum and mitochondria in various muscles: a review. *Scanning Microsc.* 7, 145–156 (1993).
47. Soeller C, Cannell MB: Examination of the transverse tubular system in living cardiac rat myocytes by 2-photon microscopy and digital image-processing techniques. *Circ. Res.* 84, 266–275 (1999).

48. Frank JS: Ultrastructure of the unfixed myocardial sarcolemma and cell surface. In: *Calcium and the Heart.* Langer GA (Ed.). Raven Press, New York, USA 1–25 (1990).
49. Bers DM: *Excitation-contraction coupling and cardiac contractile force.* Kluwer Academic Publishers, Dordrecht, The Netherlands (2001).
50. Sommer JR, Johnson EA: Cardiac muscle. A comparative study of Purkinje fibers and ventricular fibers. *J. Cell Biol.* 36, 497–526 (1968).
51. Flucher BE, Franzini-Armstrong C: Formation of junctions involved in excitation-contraction coupling in skeletal and cardiac muscle. *Proc. Natl Acad. Sci. USA* 93, 8101–8106 (1996).
52. Hasenfuss G, Pieske B: Calcium cycling in congestive heart failure. *J. Mol. Cell. Cardiol.* 34, 951–969 (2002).
53. Houser SR, Margulies KB: Is depressed myocyte contractility centrally involved in heart failure? *Circ. Res.* 92, 350–358 (2003).
54. Tomaselli GF, Zipes DP: What causes sudden death in heart failure? *Circ. Res.* 95, 754–763 (2004).
55. Kubalova Z, Terentyev D, Viatchenko-Karpinski S *et al.*: Abnormal intrastore calcium signaling in chronic heart failure. *Proc. Natl Acad. Sci. USA* 102, 14104–14109 (2005).
56. Jones M, Ferrans VJ, Morrow AG, Roberts WC: Ultrastructure of crista supraventricularis muscle in patients with congenital heart diseases associated with right ventricular outflow tract obstruction. *Circulation* 51, 39–67 (1975).
57. Deshaies Y, Willemot J, Leblanc J: Protein synthesis, amino acid uptake, and pools during isoproterenol-induced hypertrophy of the rat heart and tibialis muscle. *Can. J. Physiol. Pharmacol.* 59, 113–121 (1981).
58. Su X, Sekiguchi M, Endo M: An ultrastructural study of cardiac myocytes in postmyocardial infarction ventricular aneurysm representative of chronic ischemic myocardium using semiquantitative and quantitative assessment. *Cardiovasc. Pathol.* 9, 1–8 (2000).
59. He J, Conklin MW, Foell JD *et al.*: Reduction in density of transverse tubules and L-type Ca2+ channels in canine tachycardia-induced heart failure. *Cardiovasc. Res.* 49, 298–307 (2001).
60. Song LS, Pi Y, Kim SJ *et al.*: Paradoxical cellular Ca2+ signaling in severe but compensated canine left ventricular hypertrophy. *Circ. Res.* 97, 457–464 (2005).
61. Pease DC: *Histological techniques for electron microscopy (2nd Edition).* Academic Press, New York, USA (1964).
62. Feldherr CM, Marshall JM: The use of colloidal gold for studies of intracellular exchanges in the ameba Chaos chaos. *J. Cell Biol.* 12, 640–645 (1962).
• First paper about delivery of nanogold particles into nucleus.
63. Feldherr CM: The effect of the electron-opaque pore material on exchanges through the nuclear annuli. *J. Cell Biol.* 25, 43–53 (1965).
64. Dworetzky SI, Feldherr CM: Translocation of RNA-coated gold particles through the nuclear pores of oocytes. *J. Cell Biol.* 106, 575–584 (1988).
65. Feldherr CM, Akin D: EM visualization of nucleocytoplasmic transport processes. *Electron Microsc. Rev.* 3, 73–86 (1990).
66. Feldherr CM, Akin D, Cohen RJ: Regulation of functional nuclear pore size in fibroblasts. *J. Cell Sci.* 114, 4621–4627 (2001).
67. Franzini-Armstrong C: Studies of the triad. II. Penetration of tracers into the junctional gap. *J. Cell Biol.* 49, 196–203 (1971).
68. London E: The molecular formula and proposed structure of the iron-dextran complex, imferon. *J. Pharm. Sci.* 93, 1838–1846 (2004).
69. Mannella CA: Conformational changes in the mitochondrial channel protein, VDAC, and their functional implications. *J. Struct. Biol.* 121, 207–218 (1998).
• This paper is from the laboratory studying the ultrastructure of mitochondria.
70. Feldherr CM: The intracellular distribution of ferritin following microinjection. *J. Cell Biol.* 12, 159–167 (1962).
71. Richter GW: The cellular transformation of injected colloidal iron complexes into ferritin and hemosiderin in experimental animals; a study with the aid of electron microscopy. *J. Exp. Med.* 109, 197–216 (1959).
72. Salnikov V, Lukyanenko YO, Frederick CA, Lederer WJ, Lukyanenko V: Probing the outer mitochondrial membrane in cardiac mitochondria with nanoparticles. *Biophys. J.* 92, 1058–1071 (2007).
73. Yang F, Moss LG, Phillips Jr GN: The molecular structure of green fluorescent protein. *Nat. Biotechnol.* 14, 1246–1251 (1996).
74. Huang WY, Aramburu J, Douglas PS, Izumo S: Transgenic expression of green fluorescence protein can cause dilated cardiomyopathy. *Nat. Med.* 6, 482–483 (2000).
•• Describes problems for cardiac functioning resulting from the overexpression of proteins.
75. Kotlikoff MI: Genetically encoded Ca2+ indicators: using genetics and molecular design to understand complex physiology. *J. Physiol.* 578, 55–67 (2007).
• Describes fluorescent nanostructures that could be produced by cells.
76. Colombini M: VDAC: the channel at the interface between mitochondria and the cytosol. *Mol. Cell. Biochem.* 256/257, 107–115 (2004).
• This paper is written by the scientist who discovered the channel.
77. Carneiro CM, Merzlyak PG, Yuldasheva LN *et al.*: Probing the volume changes during voltage gating of Porin 31BM channel with nonelectrolyte polymers. *Biochim. Biophys. Acta* 1612, 144–153 (2003).
78. Ufret-Vincenty CA, Baro DJ, Lederer WJ *et al.*: Role of sodium channel deglycosylation in the genesis of cardiac arrhythmias in heart failure. *J. Biol. Chem.* 276, 28197–28203 (2001).
79. De Brabander M, Geuens G, Nuydens R *et al.*: Probing microtubule-dependent intracellular motility with nanometre particle video ultramicroscopy (nanovid ultramicroscopy). *Cytobios.* 43, 273–283 (1985).
80. Pastorino JG, Hoek JB: Hexokinase II: the integration of energy metabolism and control of apoptosis. *Curr. Med. Chem.* 10, 1535–1551 (2003).
81. Vyssokikh M, Brdiczka D: VDAC and peripheral channelling complexes in health and disease. *Mol. Cell. Biochem.* 256, 117–126 (2004).
82. Bustamante JO, Michelette ER, Geibel JP *et al.*: Dendrimer-assisted patch-clamp sizing of nuclear pores. *Pflugers Arch.* 439, 829–837 (2000).
83. Day SM, Westfall MV, Fomicheva EV *et al.*: Histidine button engineered into cardiac troponin I protects the ischemic and failing heart. *Nat. Med.* 12, 181–189 (2006).
•• First nanomedical paper relevant to real therapeutic effect of genes delivered into cardiac cells.
84. Verma DD, Levchenko TS, Bernstein EA *et al.*: ATP-loaded immunoliposomes specific for cardiac myosin provide improved protection of the mechanical functions of myocardium from global ischemia in an isolated rat heart model. *J. Drug Target.* 14, 273–280 (2006).
85. Gazitt Y, Loyter A, Ohad I: Induction of ATP depletion, intramembrane particle aggregation and exposure of membrane

phospholipids in chicken erythrocytes by local anesthetics and tranquilizers. *Biochim. Biophys. Acta.* 471, 361–371 (1977).

86. Van der Ende A, du Maine A, Schwartz AL, Strous GJ: Effect of ATP depletion and temperature on the transferrin-mediated uptake and release of iron by BeWo choriocarcinoma cells. *Biochem. J.* 259, 685–692 (1989).
87. Mandel LJ, Doctor RB, Bacallao R: ATP depletion: a novel method to study junctional properties in epithelial tissues. II. Internalization of Na+,K+-ATPase and E-cadherin. *J. Cell Sci.* 107, 3315–3324 (1994).
88. Bacher CP, Reichenzeller M, Athale C *et al.*: 4-D single particle tracking of synthetic and proteinaceous microspheres reveals preferential movement of nuclear particles along chromatin – poor tracks. *BMC Cell Biol.* 5, 45–59 (2004).
89. Choi WS, Khurana A, Mathur R *et al.*: Kv1.5 surface expression is modulated by retrograde trafficking of newly endocytosed channels by the dynein motor. *Circ. Res.* 97, 363–371 (2005).
90. Blanchard E, Belouzard S, Goueslain L *et al.*: Hepatitis C virus entry depends on clathrin-mediated endocytosis. *J. Virol.* 80, 6964–6972 (2006).
91. Choi SY, Huang P, Jenkins GM *et al.*: A common lipid links Mfn-mediated mitochondrial fusion and SNARE-regulated exocytosis. *Nat. Cell Biol.* 8, 1255–1262 (2006).
92. Meeusen S, DeVay R, Block J *et al.*: Mitochondrial inner-membrane fusion and crista maintenance requires the dynamin-related GTPase Mgm1. *Cell* 127, 383–395 (2006).
93. Gorelik J, Gu Y, Spohr HA *et al.*: Ion channels in small cells and subcellular structures can be studied with a smart patch-clamp system. *Biophys. J.* 83, 3296–3303 (2002).
94. Lukyanenko V, Ziman A, Lukyanenko A *et al.*: Functional groups of ryanodine receptors in rat ventricular cells. *J. Physiol.* 583(Pt 1), 251–269 (2007).